The effects of nicotine replacement on cognitive brain activity during smoking withdrawal studied with simultaneous fMRI/EEG

John D. Beaver, Christopher J. Long, David M. Cole, Michael J. Durcan, Linda C. Bannon, Rajesh G. Mishra, Paul M. Matthews

The effects of nicotine replacement on cognitive brain activity during smoking withdrawal studied with simultaneous fMRI/EEG

John D. Beaver, PhD[*1], Christopher J. Long, PhD[1], David M. Cole, MSc[1,2], Michael J. Durcan, PhD[3], Linda C. Bannon, BSc[3], Rajesh G. Mishra, MD, PhD[3], Paul M. Matthews, MD, DPhil[1,2]

1. GlaxoSmithKline Clinical Imaging Centre, Hammersmith Hospital, London, UK.
2. Department of Clinical Neuroscience, Imperial College, London, UK.
3. GlaxoSmithKline Consumer Healthcare, Weybridge, UK.

Corresponding author

Dr John Beaver

GSK Clinical Imaging Centre

Hammersmith Hospital — Tel: +44 (0) 208 008 6014

Du Cane Road — Fax: +44 (0) 208 008 6491

London W12 0NN, UK — Email: j.beaver@cantab.net

Running title: Nicotine effects on cognitive brain activity

ABSTRACT

Impaired attention ("difficulty concentrating") is a cognitive symptom of nicotine withdrawal that may be an important contributor to smoking relapse. However, the neurobiological basis of this effect and the potentially beneficial effects of nicotine replacement therapy both remain unclear. We used functional MRI with simultaneous electroencephalogram (EEG) recording to define brain activity correlates of cognitive impairment with short-term smoking cessation in habitual smokers and the effects of nicotine replacement. We found that irrespective of treatment (i.e., nicotine or placebo) EEG alpha power was negatively correlated with increased activation during performance of a rapid visual information processing (RVIP) task in dorsolateral prefrontal, dorsal anterior cingulate, parietal, and insular cortices, as well as, caudate, and thalamus. Relative to placebo, nicotine replacement further increased the alpha-correlated activation across these regions. We also found that EEG alpha power was negatively correlated with RVIP- induced deactivation in regions comprising the "default mode" network (i.e., angular gyrus, cuneus, precuneus, posterior cingulate and ventromedial prefrontal cortex). These alpha-correlated deactivations were further reduced by nicotine. These findings confirm that effects of nicotine on cognition during short-term smoking cessation occur with modulation of neuronal sources common to the generation of both the BOLD and alpha EEG signals. Our observations thus demonstrate that nicotine replacement in smokers has direct pharmacological effects on brain neuronal activity modulating cognitive networks.

Keywords: Nicotine, Cognitive impairment, Smoking, Addiction, fMRI, EEG

INTRODUCTION

Over 1 billion people currently smoke tobacco and half of all long-term smokers die from smoking-related illnesses (Royal College of Physicians, 2007). However, nicotine dependence is difficult to treat. Only 5-7% of unassisted attempts to stop smoking are successful for more than 6 months; multiple attempts typically are necessary to achieve long-term abstinence (Hughes, Peters, & Naud, 2008). Mild cognitive impairments such as difficulty concentrating are an established symptom of nicotine withdrawal, and may be an important trigger for smoking relapses (Parrott & Roberts, 1991; Parrott, Garnham, Wesnes, & Pincock, 1996). Furthermore, anticipation of these symptoms adds to the challenge of initiating repeat attempts at cessation. Previous research has demonstrated that nicotine replacement is effective in reversing withdrawal-induced performance deficits on cognitive tests of sustained attention and working memory (Atzori, Lemmonds, Kotler, Durcan, & Boyle, 2008). However, the specific pharmacodynamic mechanisms of nicotine responsible for this clinically important treatment effect have not been defined.

Functional magnetic resonance imaging (fMRI) of smokers suggests that nicotine replacement prior to the onset of withdrawal modulates brain activity during cognitive task performance in regions previously implicated in arousal, attention, and working memory. For example, (Lawrence, Ross, & Stein, 2002) showed that applying a nicotine patch to minimally abstinent smokers results in increased blood oxygen level dependent (BOLD) signal in the parietal cortex, caudate, and thalamus during performance of a rapid visual information processing (RVIP) task, and reduced BOLD response in parahippocampal gyrus and insula. More recent fMRI studies of nicotine replacement prior to withdrawal onset have shown that nicotine replacement is also associated with decreased BOLD response in regions of the so-called “default mode” network and thalamus (Hahn et al., 2007; Hahn et al., 2009). However, whether nicotine replacement following withdrawal onset changes cognitive brain activity was not made clear by these initial studies.

In addition, functional MRI does not measure neuronal activity directly, but is based on the interaction between vascular responses and local tissue oxidative metabolism (Ogawa, Lee, Kay, & Tank, 1990). A critical concern for all pharmacological fMRI studies is the possibility that BOLD responses may be induced by non-neuronal drug effects (e.g., alterations in neurovascular coupling), rather than drug-induced changes in neuronal activity (Iannetti & Wise,

2007a; Matthews, Honey, & Bullmore, 2006b). This may be particularly important for studies of agents like nicotine, which can have direct pharmacological effects on cerebral vasculature (Iida et al., 1998). Several previous fMRI studies of nicotine's effects on cognition have attempted to address this issue by demonstrating the absence of treatment effects on resting cerebral blood flow (as assessed with arterial spin labelling) and regional BOLD signal during a control activation task (Hahn et al., 2007; Hahn et al., 2009).

To assess brain activity related to cognitive enhancement by nicotine replacement in withdrawal, we used BOLD fMRI with simultaneous electroencephalographic (EEG) recording while abstinent smokers performed an RVIP task. Integration of the EEG, which provides a direct electrophysiological measure of neuronal activity, with fMRI increased confidence that signals measured with the latter reflected true neuronal responses. Prior to each fMRI scan, participants were deprived of cigarettes for 8 hrs before being dosed with nicotine or placebo lozenges in a double-blind, crossover design. We hypothesized that task-related modulation of the BOLD signal would be inversely correlated with EEG alpha power in brain regions previously implicated in sustained attention, executive function and working memory, as well as regions of the default network. We further hypothesised that (relative to placebo) nicotine replacement during smoking withdrawal would potentiate the alpha-correlated BOLD activity in each of these regions.

METHODS

Participants. We enrolled 23 right-handed, adult smokers, with no history of neurological/psychiatric illness (confirmed in writing by their GP) or current drug use (other than tobacco smoking). Participants smoked regularly for at least three years, smoked an average of 15 commercially available cigarettes per day, and normally consumed a cigarette within 30 minutes of waking. Data from eight participants did not pass both fMRI and EEG quality control checks (see Data analysis), and therefore all data from these subjects were excluded from analysis. For the final pool of 15 participants (4 female; mean age = 30.3 years ± 7.7 (SD), range = 21-49 years), scores on the Fagerström Test for Nicotine Dependence (Heatherton et al., 1991) were 5.1 ± 1.5 (Mean ± SD). All participants gave written, informed consent and the protocol was approved by the Charing Cross Hospital Research Ethics Committee, London, UK.

Study design. Each participant underwent screening followed by two treatment visits in a randomised, placebo-controlled, crossover design with at least 48 hr between treatment visits. Participants received either 4mg nicotine lozenges (NiQuitin CQ®, GlaxoSmithKline), or taste-matched placebo lozenges containing capsicum at each visit.

A detailed sequence of events at each treatment visit is presented in Supplementary Table 1. At each visit participants arrived at the clinic at approximately 06:30AM. Under supervision, participants smoked one cigarette and then abstained from smoking for 8 hr before the first dosing and thereafter until the end of the session. Subjects completed a computerised RVIP task approximately 60 minutes prior to the first dose administration to minimise possible practice effects. This task was administered inside the scanner while it was not active to acclimatize volunteers to the scanning environment prior to actual data collection. Subjects were subsequently dosed with either the 4 mg nicotine lozenge or placebo at time 0 and then again after 2 hrs. Previous behavioural studies in smokers have shown that the 4mg nicotine lozenge dosed in this way significantly improves withdrawal-induced performance deficits on an RVIP task (Atzori et al., 2008). Immediately prior to both dose administrations, subjects were asked to complete subjective ratings of nicotine withdrawal and cigarette craving using the Modified Minnesota Withdrawal Symptom (MMWS) scale (Hughes & Hatsukami, 1986, Heatherton). Simultaneous fMRI/EEG data acquisition during performance of the computerised RVIP task began approximately 60 mins following the final dosing, and lasted for approximately 28 mins. After being removed from the MR scanner, subjects again completed subjective ratings of nicotine withdrawal and cigarette craving using the MMWS.

Cognitive task. The cognitive task consisted of a series of centrally displayed, single numbers (0-9) back-projected into the bore of the scanner at a rate of 100 per minute. During RVIP blocks, participants identified sequences of three consecutive odd or even numbers from a pseudo-random sequence by pressing the corresponding button on a response box as quickly as possible. During control (CNTRL) blocks, participants identified single occurrences of the number “0”. The number and position of targets within each block were matched and counterbalanced across block type. Each block lasted 90sec and there were 8 blocks of each type in total, presented in counterbalanced order. A 30sec rest block was presented after every two consecutive blocks

during which participants were instructed to fixate a centrally displayed (+) symbol. The dependent variables were accuracy (number of correctly identified targets/total number of targets) and response time (the average response time in milliseconds to correctly identify targets).

fMRI acquisition. At each visit, single-shot, T2*-weighted, gradient-echo planar imaging (EPI) sensitive to BOLD contrast was carried out during performance of the task on a 3-Tesla MAGNETOM TIM Trio whole-body MRI scanner (Siemens, Erlangen, Germany) with a 12-channel birdcage radio frequency head coil. Images were collected in one continuous run of 548 volumes. Whole-brain images were acquired in 41-slices (TR = 3000 ms, TE = 30 ms, flip angle = 90º, voxel size = 3.5 mm isotropic). The first 4 volumes were discarded to allow for magnetic equilibration. Additional high-resolution T1-weighted anatomical MRI scans (MPRAGE) were acquired for each subject to aid with EPI co-registration (TR = 3000 ms, TE = 3.66 ms, flip angle = 9º, voxel size = 1 mm isotropic, 208 slices).

EEG acquisition. EEG was continuously recorded inside the MRI scanner during task performance using the MRI-compatible BrainAmp system (Brainproducts, GmbH Germany). We recorded from 32 scalp sites positioned according to 10–20 system (including channels O_1, O_2, P_3, P_4 used in alpha analyses) with the average of mastoid channels TP_1 and TP_2 used as a reference node. The "BrainCap" (BrainProducts, GmbH Germany) MRI compatible sintered Ag/AgCl ring electrodes were placed in contact with the scalp using MR compatible conductive electrolyte gel around the electrodes. Electrode impedance was kept below 10KΩ. An electrode was placed on the infra-orbital ridge of the right eye to record vertical EOG. The BrainProducts BrainAmp ExG system was used to measure high SNR bipolar electrocardiograms (ECGs) to capture cardiac dynamics. All data (EEG and ECG) were digitised through amplifiers with the following specifications: 1000Hz low-pass filter, 10s (time constant) high pass filter, with a 5000 Hz sampling rate and a 16-Bit analogue to digital quantization resolution featuring a dynamic range of ± 600 mV. The EEG amplifier was placed directly behind the head coil inside the scanner bore, and connected by fibre optic to the recording and analysis computer located in the control room. The ECG amplifier was placed at the foot of the scanner with the cables routed to be approximately parallel to the system Gauss lines, avoiding the head coil entirely. Both amplifiers were weighted with sandbags to mitigate the effects of gradient-induced vibration. We

synchronized the EEG amplifier clock with the 10MHz master clock of the TIM Trio system to record EEG and ECG in phase with MRI gradient switching.

Data analysis

EEG Preprocessing. We used Brain Vision Analyzer (Brainproducts, GmbH Germany) to perform off-line correction of gradient imaging and ECG artefacts as described previously (Allen, Polizzi, Krakow, Fish, & Lemieux, 1998; Allen, Josephs, & Turner, 2000). A detailed description of our EEG pre-processing procedure is provided in the Supplementary Materials. The EEG data were manually inspected to assess the efficacy of the pre-processing. Data from eight participants were discarded due to significant corruption of more than 20% of the EEG or failure to successfully remove artefacts. For the remaining 15 subjects, we derived alpha power time-courses by computing the Power Spectral Density (PSD) using a fast Fourier transform (FFT) with a windowing width corresponding to the fMRI TR (3s). The spectral alpha power was derived for each TR by integrating the PSD within the alpha frequency band (~ 8-12 Hz).

fMRI preprocessing. fMRI data were analysed with FSL version 4.1 (www.fmrib.ox.ac.uk/fsl/). Individual sessions with mean head motion exceeding the in-plane size of a voxel (3mm) were excluded (incidentally, these sessions were restricted to subjects who were discarded due to poor quality EEG data). Data were high-pass filtered, spatially smoothed (6mm Full Width Half Maximum Gaussian kernel), and corrected for motion using a rigid body transformation to align each image in the series with the mid-image of the run. Further pre-processing included grand mean intensity normalisation of the entire 4D dataset by a single scaling factor.

Integration of EEG and fMRI data. The approach we used here attempts to build on earlier correlation approaches originally utilised to explore the relationship between EEG alpha power timecourses and BOLD signals at rest (e.g., (Laufs et al., 2003). In general, a correlation score computed between two signals reflect only temporal synchronicity, independent of possible changes in amplitude. We therefore employed a regression-based model to capture both synchronicity and amplitude. Sensitivity to amplitude is critical to our present work because we employed a cognitive task designed to experimentally manipulate the signal amplitude. This

approach also contrasts with previous investigations that examined correlative EEG/fMRI relationships on subjects at rest.

Building upon standard fMRI time-series approaches (Smith, 2004), we combined the estimated EEG alpha power dynamics with empirical observations about the nature and form of the fMRI noise $w_{t,v}$ culminating in the following model for the time-course at each location in the brain. That is, we used the model $x_{t,v} = m_v + s_{t,v}^{Alpha} + w_{t,v}$ to integrate EEG alpha signal with fMRI data at each voxel, *v,* in the brain, where m_v is the signal mean and the observed timecourses have been treated for low-frequency nuisance effects by a weighted running lines smoother (Woolrich, Beckmann, Nichols, & Smith, 2009a). $w_{t,v}$ was a serially correlated first-order autoregressive stochastic noise component present to capture physiological fluctuations in the data not related to the task design. Since we operate on the assumption that EEG alpha power directly correlates with the fMRI BOLD signal (Laufs et al., 2003), we can decouple the alpha signal $s_{t,v}$ into two components: (a) a steady state or mean signal to capture the task design, c_t, and (b) residual amplitude fluctuations in the brain response reflected by changes in the alpha power curve. We decomposed $s_{t,v}^{Alpha}$ into its task-related (constant) component and the EEG-derived variations about this constant component as follows: $s_{t,v}^{Alpha} = \bar{s}_{t,v} + \tilde{s}_{t,v}$ (see Supplementary Figure 2), with the steady state component of the EEG proportional to the standard fMRI block response $\bar{s}_{t,v} = H(t - D_v)\left(g_{v,t} * c_{t-D_v}\right)$. D_v was a hemodynamic delay of 6s and H was a Heaviside step function. The hemodynamic response $g_{v,t}$ was characterised by a discrete gamma function with a dispersion constant (sd=3s). Next, we computed the alpha power fluctuation $\tilde{s}_{.,v}$ about the steady-state $\bar{s}_{.,v}$ by fitting the observed alpha power curve $s_{t,v}^{Alpha}$ onto the fMRI model such that $\bar{s}_{.,v} \perp \tilde{s}_{.,v}$. Specifically these power fluctuations can be computed as the residuals of the fitted linear model. That is, $\tilde{s}_{t,v} = s_{t,v}^{Alpha} - \gamma \bar{s}_{t,v}$, where the scaling factor γ is derived as a natural by-product of this linear model-based orthogonalization. That is, $\gamma = \sum_t \left(\bar{s}_{t,v} \cdot s_{t,v}^{Alpha}\right) / \sum_t \left(\bar{s}_{t,v} \cdot \bar{s}_{t,v}\right)$. This computation was performed at the start of the analysis of each session and subsequently fit at each fMRI voxel with spatially fixed γ and $\tilde{s}_{t,v}$ but with spatially varying estimates of the constant model BOLD response amplitudes, alongside the alpha power rhythm amplitudes. In summary, this approach simultaneously models amplitude fluctuations in the fMRI data related

to underlying alpha activity that complements estimations related to the steady state fMRI time-series model fit. More information on the rationale behind this approach is presented in the Supplemental Material.

Statistical analysis of fMRI/EEG data. We estimated the signal parameters at each voxel using a weighted least squares model with intrinsic correction for spatial autocorrelations (Woolrich, Beckmann, Nichols, & Smith, 2009). Experimental regressors consisted of task condition using a blocked design matrix with one column assigned to each condition (RVIP or CNTRL). Each of these columns was convolved with a predefined hemodynamic response function to imputed lag and response of the brain function to the stimulus intrinsic to the system dynamics of the neurovascular response. An additional column incorporated the orthogonalized EEG alpha power timeseries. The nuisance part of the design matrix was configured to model head motion (values derived from the initial motion correction stage), and behavioral response times to control for potential effects of nicotine on the speed of processing. Each individual statistical map was normalised into a standard reference space (the MNI-152 template) using the FMRIB linear image registration tool (FLIRT) for comparison across individuals. At the individual level, Z-statistic images were thresholded at cluster significance threshold of $P<0.05$ (whole-brain corrected for multiple comparisons).

Group mixed-effects analyses were then performed to produce *Z* (Gaussianized T/F) statistic images corrected for multiple comparisons using Gaussian Random Field Theory-based maximum height thresholding, with a corrected significance threshold of $P < 0.005$. In all figures, activation maps are shown overlaid on the MNI-152 high-resolution image. To test the effects of nicotine on task-related activity, we created functionally-defined regions of interest (ROIs) for the contrast RVIP - CNTRL (rest periods were not analyzed). In task-related regions specified in this way, we recorded for the task conditions, in each region, and each subject, the mean percent BOLD change within the mask. This procedure simplified the data analysis by overall reduction of the magnitude of the multiple testing problems of whole-brain approaches, while allowing for inter-subject variability in the exact area of activation (while still constraining each ROI's response to a specific mask).

Functionally defined ROI masks may potentially bias the resulting inferences unless the contrast generating the masks is statistically independent from the contrast of interest. Therefore,

we ensured independence by computing initial ROI masks based on a mixed-effects group analysis collapsed across both visits (that is, by accounting for the nicotine and placebo treatment effect in the mixed-effects statistical model). This 2-dose average is therefore independent to our main comparison of interest (i.e., Nicotine vs. Placebo), and hence will not bias our results.

The statistical maps were divided into anatomical regions using the Harvard-Oxford atlas (Harvard Center for Morphometric Analysis) to label and constrain clusters of activated voxels to anatomical regions. These ROIs were then applied to each individual subject's fMRI data and the mean regional percent BOLD signal change was extracted during task performance on each dosing visit. For the main contrasts of interest (RVIP - CNTRL), we assessed significance by using a corrected maximum height α-level of 0.005.

RESULTS

Behavioural measures. Nicotine withdrawal was assessed using the MMWS scale once prior to dosing and again immediately after the fMRI scan. The post-dose assessment corresponded to 1.75 hr (±30 mins) after the second dose and 11.75 hr (±30 mins) after the subject's last cigarette. The mean pre-dose MMWS scores were 8.0 (±1.02SE) and 8.5 (±0.78SE) for the nicotine and placebo visits, respectively ($t(14) < 1$, NS). Paired t-test of the post-dose MMWS scores showed that the subjective experience of withdrawal was significantly lower following nicotine lozenge relative to placebo ($t(14)=2.43$, $p<.02$) (Figure 1). There was also a significant effect of nicotine on RVIP accuracy, with significantly greater accuracy following nicotine compared with placebo ($t(14)=2.61$, $p<.02$, Figure 2). Furthermore, response times to correctly identify target RVIP sequences were significantly faster for nicotine compared with placebo ($t(14)=3.33$, $p<.005$; Figure 2). We did not find a significant difference in accuracy between nicotine and placebo visits for the control task ($t<1$), but there was a near-significant trend towards faster response times following nicotine ($t(14)=3.33$, $p=.0512$). This was expected because the control task was designed to place low attentional/cognitive demands on participants, resulting in so-called 'ceiling effects' in which participants perform very well irrespective of treatment with little room for improvement.

EEG alpha. We fit the processed alpha time-course data to the task model (as shown in Supplemental Figure 1) for each subject and session to compute the mean alpha power spectral density during RVIP performance. Paired t-tests confirmed that the mean alpha power during

RVIP was significantly attenuated following nicotine replacement compared with placebo ($t(14)=-1.77$, $P < 0.05$)

Combined fMRI/EEG data.

Identification of RVIP-related activity. For the contrast RVIP - CNTRL collapsed across both treatment sessions, we identified six regions showing significant *increased* activation negatively correlated with EEG alpha power. Regions of significant increased activation included the bilateral caudate (X_{max}=-10, Y_{max}=-2, Z_{max}=10, z_{max}=6.091, nVOX= 75), dorsal anterior cingulate cortex (X_{max}=8, Y_{max}=18, Z_{max}=36, z_{max}=10.62, nVOX=552), dorsolateral prefrontal cortex (X_{max}=-44, Y_{max}=6, Z_{max}=34, z_{max}=14.47, nVOX=2860), insula (X_{max}=-34, Y_{max}=18, Z_{max}=0, z_{max}=9.649, nVOX=332), parietal lobule (X_{max}=24, Y_{max}=-58, Z_{max}=42, z_{max}=14.11,nVOX=3379), and thalamus (X_{max}=-8, Y_{max}=-16, Z_{max}=6, z_{max}=8.845, nVOX=249) (Figure 3A). In each of these regions, *increased* BOLD response during performance of the RVIP task was associated with *reduced* alpha power. Supplementary Figure 3 presents an example time-course plot depicting the close correlation of the BOLD fMRI and alpha EEG signals in the dorsal anterior cingulate of a single participant.

We also identified five regions showing significant *decreased* activation (for the RVIP – CNTRL contrast) negatively correlated with alpha power. These regions included angular gyrus (X_{max}=-42, Y_{max}=-68, Z_{max}=22, z_{max}=-6.112, nVOX=1770), cuneus (X_{max}=0, Y_{max}=-82, Z_{max}=24, z_{max}=-4.244, nVOX=354), ventromedial prefrontal cortex (X_{max}=-2, Y_{max}=50, Z_{max}=-8, z_{max}=-4.573, nVOX=218), precuneus (X_{max}=-8, Y_{max}=-60, Z_{max}=10, z_{max}=-5.336, nVOX=1221), and posterior cingulate (X_{max}=12, Y_{max}=-50, Z_{max}=30, z_{max}=-5.640, nVOX=1311), which, together, correspond to the so-called "default mode" network identified in resting state fMRI studies (De Luca, Beckmann, De Stefano, Matthews, & Smith, 2006b) (Figure 3A). In each of these regions, *decreased* BOLD response during performance of the RVIP task was associated with *heightened* alpha power.

Effects of nicotine replacement on RVIP-related activity. Our primary hypothesis was that nicotine replacement during short-term smoking cessation would increase activity in regions of interest showing alpha-correlated activation during the RVIP-task (i.e., caudate, dorsal anterior cingulate, dorsolateral prefrontal cortex, insula, parietal lobule, and thalamus). To test this, we

entered the mean alpha-correlated BOLD signal change for the RVIP – CNTRL contrast from these regions into a 2 x 6 repeated measures ANOVA, with treatment (nicotine vs. placebo) and ROI as independent variables. We used bilateral ROIs since the regions identified in the RVIP analysis above were bilateral. The results showed significant main effects of treatment ($F(1,14) = 6.09$; $P < 0.05$) and ROI ($F(1,14) = 6.70$; $P < 0.01$). Importantly, there was no significant interaction between the two ($F(1,14) = 1.41$; $P > 0.20$). Confirming our first hypothesis, alpha-correlated activation was significantly increased by nicotine compared with placebo (mean % signal change = 0.577 and 0.405, respectively) across these regions. For completeness, we also carried out post-hoc paired t-tests which confirmed that alpha-correlated activation was significantly increased by nicotine within each of these ROIs (all $P < 0.05$) except the parietal lobule ($P > 0.2$). Figure 3B shows the mean signal change for the RVIP – CNTRL contrast in each region.

A related hypothesis was that nicotine replacement would further reduce activity in regions showing alpha-correlated deactivation during RVIP performance (i.e., angular gyrus, cuneus, precuneus, posterior cingulate, and ventromedial prefrontal cortex). We tested this hypothesis by entering the mean alpha-correlated BOLD signal change for the RVIP – CNTRL contrast from the bilateral ROIs into a 2 x 5 repeated measures ANOVA, with treatment and ROI as independent variables. The results showed significant main effects of treatment ($F(1,14) = 8.43$; $P < 0.02$) and ROI ($F(1,14) = 11.06$; $P < 0.005$), but no significant interaction between the two ($F(1,14) = 1.41$; $P > 0.20$). Confirming our second hypothesis, alpha-correlated deactivations in these regions were further reduced by nicotine relative to placebo (mean % signal change = -0.572 and -0.364, respectively). Post-hoc paired t-tests confirmed that this effect was significant in each of these regions (all $P < 0.05$) except the precuneus, in which a trend was observed ($P < 0.09$). For each region of deactivation, the mean signal change for the RVIP – CNTRL contrast is presented in Figure 3C.

DISCUSSION

We used fMRI with simultaneous EEG recording to investigate changes in brain activity related to cognitive enhancement by nicotine replacement therapy during short-term smoking withdrawal. We found that nicotine replacement was associated with reduced subjective experience of withdrawal symptoms (as assessed by the MMWS) and improved target

identification during performance of a demanding rapid visual information processing task, consistent with previous behavioural findings (Atziori et al., 2008). At the level of neural networks, we found negative correlations between task-related BOLD *increases* and EEG alpha power in the thalamus, caudate, anterior insula, parietal lobule, dorsal ACC and DLPFC. In support of our primary hypothesis, nicotine replacement during smoking withdrawal potentiated the alpha-correlated BOLD activity in each of these regions, except parietal lobule. We also found negative correlations between task-induced BOLD *decreases* (i.e., task-related deactivation) and EEG alpha power in regions comprising the "default mode" network (including the posterior cingulate, precuneus, angular gyrus and ventromedial prefrontal cortex (see De Luca, Beckmann, De Stefano, Matthews, & Smith, 2006). Nicotine replacement also potentiated these alpha-correlated deactivations, showing that nicotine suppresses markers of a "resting" state, consistent with greater task-specific attention (Hahn et al., 2007). Together, these results demonstrate that relevant brain networks subserving cognition and attention are pharmacologically modulated directly by nicotine replacement after smoking cessation. These findings provide a neurobiological rationale for use of nicotine replacement to manage cognitive symptoms of smoking cessation in habitual smokers.

We integrated fMRI with EEG to increase confidence that BOLD changes arose from modulation of neuronal activity, rather than from direct effects on vascular response (Iannetti & Wise, 2007; Matthews, Honey, & Bullmore, 2006). To our knowledge this is the first pharmacological fMRI study to employ concurrent recording of EEG. This approach is particularly important for fMRI studies of nicotine, which has well known sympathomimetic properties (Perkins et al., 2004; Yugar-Toledo et al., 2005) and can have direct effects on neurovascular coupling (Toda, 1975; Boyajian and Otis, 2000; Sabha et al., 2000). EEG alpha power fluctuations provide an electrophysiological index of rhythmic changes in the relative level of depolarization in somatic and dendritic membrane potentials of masses of neurons (Klimesch, Sauseng, & Hanslmayr, 2007). Although fMRI has high spatial resolution, the BOLD signal has only an indirect relationship with neuronal activity. Scalp EEG on the other hand lacks the spatial resolution of fMRI, but provides a more direct, electrophysiological index of underlying neuronal activity. Because these two imaging modalities provide complementary data, their combination affords a stronger basis for interpreting nicotine's effects on the BOLD response in neuronal terms. In accordance with the present findings, previous research has shown

that performance of demanding cognitive tasks is associated with reduced power in the EEG alpha frequency band, and nicotine administration in abstinent smokers has been shown to reduce alpha power (Domino et al., 2009). At the neuronal level, low alpha power reflects states of relatively high excitatory activity (Klimesch, Sauseng, & Hanslmayr, 2007), and in line with the current findings previous simultaneous fMRI-EEG studies have reported negative correlations between alpha power and spontaneous fluctuations in BOLD activity in frontal, parietal and thalamic regions (Goldman et al., 2002; Laufs et al., 2003; De Munck, Gonτalves, Mammoliti, Heethaar, & Lopes da Silva, 2009).

In the context of demonstrable performance effects of nicotine replacement, the close temporal correspondence between the BOLD and electrophysiological signals provides strong evidence that the improvements in behavior observed here are related to neuronal sources common to the EEG and fMRI signals. Evidence from neurophysiology studies across a number of species including non-human primates suggests that the neuronal processes that give rise to local field potentials are a likely common factor between these two modalities (Goense & Logothetis, 2008; Kayser, Kim, Ugurbil, Kim, & Konig, 2004; Logothetis, Pauls, Augath, Trinath, & Oeltermann, 2001). Although fMRI provides localization of the underlying neuronal sources with greater functional anatomical precision than is possible with EEG alone (Goldman, Stern, Engel, & Cohen, 2000; Goldman et al., 2002; Laufs et al., 2003), the fMRI signal does not distinguish between regions that are modulated directly and those that show neuronal activity changes through secondary afferent activity (Schwarz et al., 2004). It is important to note that the present approach to integrating fMRI and EEG data is not an attempt to identify the neural generators of the EEG alpha signal *per se*.

Not all brain regions showing task-specific modulation showed increased activation after nicotine replacement. Although nicotine is associated with excitation post-synaptically, nicotine enhances both glutamatergic and GABAergic pathways pre-synaptically (Mansvelder, Keath, & McGehee, 2002). For example, nicotinic acetylcholine receptors located on GABAergic interneurons known to inhibit pyramidal neurons may provide one pathway via which nicotine can influence network oscillations. Our observations do not allow us to distinguish between nicotine replacement's effects on neuronal excitation or inhibition *per se*. Rather, they more generally support the conclusion that the effects of nicotine replacement on cognitive task

performance in smokers are associated with localised changes in the relative balance between excitatory and inhibitory activity.

Previous functional imaging investigations in smokers and non-smokers have reported patterns of modulation involving both activation and deactivation following nicotine administration (Hahn et al., 2007; Hahn et al., 2009; Lawrence, Ross, & Stein, 2002; Sweet et al., 2010; Thiel, Zilles, & Fink, 2005; Vossel, Thiel, & Fink, 2007). Here we have built on observations in this study and in previous work to distinguish two large classes of response. We found increased activity in regions known to be involved in sustained attention, executive control and working memory, and decreased activity in brain regions constituting the default mode network. Increased task-related activations in the caudate and thalamus are generally in accord with Lawrence et al. (2002), who observed a similar pattern of results during RVIP performance following nicotine replacement in non-abstinent smokers (see below for discussion of differences). Our finding that nicotine further reduced task-related deactivations in regions comprising the default network is compatible with several more recent studies of nicotine replacement in non-abstinent smokers (Hahn et al., 2007; Hahn et al., 2009). What our study uniquely contributes is the integration of these findings in the clinically important context of abstinent smokers after short-term nicotine withdrawal.

We also found that nicotine replacement increased RVIP-related activity in dorsolateral prefrontal and dorsal anterior cingulate regions but not in the parietal lobule, which is in contrast to Lawrence et al. (2002). The dorsolateral prefrontal cortex plays a key role in working memory and executive function (Procyk & Goldman-Rakic, 2006), mediated in part through direct anatomical connectivity with the dorsal anterior cingulate and medial thalamus (Behrens et al., 2003; Carter & van Veen, 2007). One potential explanation for the differences between our findings and those of Lawrence et al. (2002) may be that sensitivity to the effects of nicotine on this functional network may have been increased in our study because we restricted our analysis to regions where task-related activity was significantly correlated with EEG alpha power. This explanation is congruent with evidence suggesting that the thalamus may be the central generator of alpha waves (Klimesch, Sauseng, & Hanslmayr, 2007) or they may arise from dendritic fields of pyramidal cells in the cortex that receive inputs from subcortical relays including the thalamus and caudate (Bollimunta, Chen, Schroeder, & Ding, 2008). A second possibility may be that even subtle task differences may elicit different patterns of neural modulation (Hahn et al., 2009).

Finally, a third possibility may be that our participants were abstinent for 8hrs prior to treatment, whereas most previous functional imaging studies of nicotine's effect on cognition in smokers administered treatment prior to withdrawal onset. However, this latter explanation seems unlikely as one such recent study reported significant nicotine-induced increases in dorsolateral prefrontal cortex activity during performance of an attention task (Hahn et al., 2007).

The present findings demonstrate that, relative to placebo, nicotine replacement improves cognitive performance and modulates cognition-related brain activity in deprived smokers, consistent with results from previous behavioural studies (Atzori et al., 2008). However, the question of whether nicotine enhances cognition or remediates a performance deficit remains a topic of debate, with some studies reporting deleterious effects of nicotine on cognition in healthy, non-smokers (Levin, McClernon, & Rezvani, 2006; Mansvelder, van Aerde, Couey, & Brussaard, 2006; Newhouse, Potter, & Singh, 2004). Nevertheless, results from several previous functional imaging studies suggest that at least under some conditions (e.g., low doses) nicotine administration in healthy, non-smokers may improve cognitive performance and modulate task-related brain activity in a number of the same regions found in the current study, including anterior cingulate and superior frontal cortex (Kumari et al., 2003; Vossel, Thiel, & Fink, 2007).

In conclusion, our results show that nicotine replacement during short-term smoking withdrawal enhances cognitive task performance and increases related brain activity in regions previously implicated in attention, executive control, and working memory, as well as decreases brain activity in regions of the default network. The close temporal correspondence between the BOLD fMRI and EEG signals across all of these regions lends confidence that these effects reflect the modulation of neuronal activity by nicotine, rather than non-neuronal effects of nicotine on cerebral blood flow or neurovascular coupling. Our findings therefore demonstrate that nicotine replacement ameliorates a negative cognitive symptom of smoking withdrawal and modulates brain cognitive networks, in addition to the well-described effects to reduce withdrawal-related nicotine craving (Shiffman et al., 2003).

Disclosure/Conflicts of Interest

This research was funded by GlaxoSmithKline, which manufactures NiQuitin CQ®. All authors were employees of GlaxoSmithKline and JDB, CJL, MJD, LCB, RGM and PMM owned shares in GlaxoSmithKline at the time the research was conducted.

Acknowledgements

We thank Ruth Hopper, Sabrina Kapur, Helen Carr, Mark Tanner, Ros Gordon, Graham Lewington and the clinical team at the GlaxoSmithKline (GSK) Clinical Imaging Centre for help with volunteer recruitment and data collection. We also thank Alex de Crespigny for physics support.

Reference List

Allen, P. J., Josephs, O., & Turner, R. (2000). A Method for Removing Imaging Artifact from Continuous EEG Recorded during Functional MRI. *NeuroImage, 12,* 230-239.

Allen, P. J., Polizzi, G., Krakow, K., Fish, D. R., & Lemieux, L. (1998). Identification of EEG Events in the MR Scanner: The Problem of Pulse Artifact and a Method for Its Subtraction. *NeuroImage, 8,* 229-239.

Atzori, G., Lemmonds, C. A., Kotler, M. L., Durcan, M. J., & Boyle, J. (2008). Efficacy of a Nicotine (4 mg)-Containing Lozenge on the Cognitive Impairment of Nicotine Withdrawal. *Journal of Clinical Psychopharmacology, 28*.

Behrens T.E.J., Johansen-Berg H., Woolrich M.W., Smith S.M., Wheeler-Kingshott C.A.M., Boulby P.A., Barker G.J., Sillery E.L., Sheehan K., Ciccarelli O., Thompson A.J., Brady J.M., Matthews P.M. (2003). Non-invasive mapping of connections between human thalamus and cortex using diffusion imaging. *Nature Neuroscience, 6,* 750–757

Bollimunta, A., Chen, Y., Schroeder, C. E., & Ding, M. (2008). Neuronal Mechanisms of Cortical Alpha Oscillations in Awake-Behaving Macaques. *Journal of Neuroscience, 28,* 9976-9988.

Carter, C. S. & Van Veen, V. (2007). Anterior cingulate cortex and conflict detection: An update of theory and data. *Cognitive, Affective, & Behavioral Neuroscience, 7,* 367-379.

De Luca, M., Beckmann, C. F., De Stefano, N., Matthews, P. M., & Smith, S. M. (2006). fMRI resting state networks define distinct modes of long-distance interactions in the human brain. *NeuroImage, 29,* 1359-1367.

De Munck, J. C., Gonτalves, S. I., Mammoliti, R., Heethaar, R. M., & Lopes da Silva, F. H. (2009). Interactions between different EEG frequency bands and their effect on alpha-fMRI correlations. *NeuroImage, 47,* 69-76.

Domino, E. F., Ni, L., Thompson, M., Zhang, H., Shikata, H., Fukai, H. et al. (2009). Tobacco smoking produces widespread dominant brain wave alpha frequency increases. *International Journal of Psychophysiology, 74,* 192-198.

Goense, J. B. M. & Logothetis, N. K. (2008). Neurophysiology of the BOLD fMRI Signal in Awake Monkeys. *Current Biology, 18,* 631-640.

Goldman, R. I., Stern, J. M., Engel, J., & Cohen, M. S. (2000). Acquiring simultaneous EEG and functional MRI. *Clinical Neurophysiology, 111,* 1974-1980.

Goldman, R. I., Stern, J. M., Engel, J. J., & Cohen, M. S. (2002). Simultaneous EEG and fMRI of the alpha rhythm. *NeuroReport, 13*.

Hahn, B., Ross, T. J., Wolkenberg, F. A., Shakleya, D. M., Huestis, M. A., & Stein, E. A. (2009). Performance Effects of Nicotine during Selective Attention, Divided Attention, and Simple Stimulus Detection: An fMRI Study. *Cerebral Cortex, 19,* 1990-2000.

Hahn, B., Ross, T. J., Yang, Y., Kim, I., Huestis, M. A., & Stein, E. A. (2007). Nicotine Enhances Visuospatial Attention by Deactivating Areas of the Resting Brain Default Network. *Journal of Neuroscience, 27,* 3477-3489.

Heatherton, T.F., Kozlowski, L.T., Frecker, R.C., Fagerström, K.O., 1991. The Fagerström test for nicotine dependence: A revision of the Fagerström tolerance questionnaire. *British Journal of Addiction, 86*, 1119-1127.

Hughes, J. R. & Hatsukami, D. (1986). Signs and Symptoms of Tobacco Withdrawal. *Archives of General Psychiatry, 43,* 289-294.

Hughes, J. R., Peters, E. N., & Naud, S. (2008). Relapse to smoking after 1áyear of abstinence: A meta-analysis. *Addictive Behaviors, 33,* 1516-1520.

Iannetti, G. D. & Wise, R. G. (2007). BOLD functional MRI in disease and pharmacological studies: room for improvement? *Magnetic Resonance Imaging, 25,* 978-988.

Iida, M., Iida, H., Dohi, S., Takenaka, M., Fujiwara, H., & Traystman, R. J. (1998). Mechanisms Underlying Cerebrovascular Effects of Cigarette Smoking in Rats In Vivo ò Editorial Comment. *Stroke, 29,* 1656-1665.

Kayser, C., Kim, M., Ugurbil, K., Kim, D. S., & Konig, P. (2004). A Comparison of Hemodynamic and Neural Responses in Cat Visual Cortex Using Complex Stimuli. *Cerebral Cortex, 14,* 881-891.

Klimesch, W., Sauseng, P., & Hanslmayr, S. (2007). EEG alpha oscillations: The inhibition-timing hypothesis. *Brain Research Reviews, 53,* 63-88.

Kumari, V., Gray, J. A., ffytche, D. H., Mitterschiffthaler, M. T., Das, M., Zachariah, E. et al. (2003). Cognitive effects of nicotine in humans: an fMRI study. *NeuroImage, 19,* 1002-1013.

Laufs, H., Kleinschmidt, A., Beyerle, A., Eger, E., Salek-Haddadi, A., Preibisch, C. et al. (2003). EEG-correlated fMRI of human alpha activity. *NeuroImage, 19,* 1463-1476.

Lawrence, N. S., Ross, T. J., & Stein, E. A. (2002). Cognitive Mechanisms of Nicotine on Visual Attention. *Neuron, 36,* 539-548.

Levin, E. D., McClernon, F. J., & Rezvani, A. H. (2-1-2006). Nicotinic effects on cognitive function: behavioral characterization, pharmacological specification, and anatomic localization. Psychopharmacology 184[3], 523-539.

Logothetis, N. K. (2008). What we can do and what we cannot do with fMRI. *Nature, 453,* 869-878.

Logothetis, N. K., Pauls, J., Augath, M., Trinath, T., & Oeltermann, A. (2001). Neurophysiological investigation of the basis of the fMRI signal. *Nature, 412,* 150-157.

Mansvelder, H., van Aerde, K., Couey, J., & Brussaard, A. (2006). Nicotinic modulation of neuronal networks: from receptors to cognition. *Psychopharmacology, 184,* 292-305.

Mansvelder, H. D., Keath, J. R., & McGehee, D. S. (2002). Synaptic Mechanisms Underlie Nicotine-Induced Excitability of Brain Reward Areas. *Neuron, 33,* 905-919.

Matthews, P. M., Honey, G. D., & Bullmore, E. T. (2006). Applications of fMRI in translational medicine and clinical practice. *Nat Rev Neurosci, 7,* 732-744.

Newhouse, P. A., Potter, A., & Singh, A. (2004). Effects of nicotinic stimulation on cognitive performance. *Current Opinion in Pharmacology, 4,* 36-46.

Ogawa, S., Lee, T. M., Kay, A. R., & Tank, D. W. (1990). Brain Magnetic Resonance Imaging with Contrast Dependent on Blood Oxygenation. *Proceedings of the National Academy of Sciences, 87,* 9868-9872.

Parrott, A. C., Garnham, N. J., Wesnes, K., & Pincock, C. (1996). Cigarette Smoking and Abstinence: Comparative Effects Upon Cognitive Task Performance and Mood State over 24 Hours. *Human Psychopharmacology: Clinical and Experimental, 11,* 391-400.

Parrott, A. C. & Roberts, G. (1991). Smoking deprivation and cigarette reinstatement: effects upon visual attention. *Journal of Psychopharmacology, 5,* 404-409.

Perkins, K. A., Lerman, C., Keenan, J., Fonte, C., & Coddington, S. (2004). Rate of nicotine onset from nicotine replacement therapy and acute responses in smokers. Nicotine Tobacco Research, 6, 501-507.

Procyk, E. & Goldman-Rakic, P. S. (2006). Modulation of Dorsolateral Prefrontal Delay Activity during Self-Organized Behavior. *Journal of Neuroscience, 26,* 11313-11323.

Royal College of Physicians (2007). Harm reduction in nicotine addiction: helping people who can't quit. *A report by the Tobacco Advisory Group of the Royal College of Physicians*. London: RCP.

Sabha, M., Tanus-Santos, J. E., Toledo, J. C. Y., Cittadino, M., Rocha, J. C., & Moreno, H. (2000). Transdermal nicotine mimics the smoking-induced endothelial dysfunction[ast]. *Clin Pharmacol Ther, 68,* 167-174.

Schwarz, A. J., Zocchi, A., Reese, T., Gozzi, A., Garzotti, M., Varnier, G. et al. (2004). Concurrent pharmacological MRI and in situ microdialysis of cocaine reveal a complex relationship between the central hemodynamic response and local dopamine concentration. *NeuroImage, 23,* 296-304.

Shiffman, S., Shadel, W. G., Niaura, R., Khayrallah, M. A., Jorenby, D. E., Ryan, C. F. et al. (2003). Efficacy of acute administration of nicotine gum in relief of cue-provoked cigarette craving. *Psychopharmacology, 166,* 343-350.

Smith, S. M. (2004). Overview of fMRI analysis. *The British Journal of Radiology, 77,* S167-S175.

Sweet, L. H., Mulligan, R. C., Finnerty, C. E., Jerskey, B. A., David, S. P., Cohen, R. A., & Niaura, R. S. (2010). Effects of nicotine withdrawal on verbal working memory and associated brain response. *Psychiatry Research Neuroimaging, 183*, 69-74.

Toda, N. (1975). Nicotine-induced relaxation in isolated canine cerebral arteries. *Journal of Pharmacology and Experimental Therapeutics, 193,* 376-384.

Thiel, C. M., Zilles, K., & Fink, G. R. (2005). Nicotine Modulates Reorienting of Visuospatial Attention and Neural Activity in Human Parietal Cortex. *Neuropsychopharmacology, 30,* 810-820.

Vossel, S., Thiel, C. M., & Fink, G. R. (2007a). Behavioral and Neural Effects of Nicotine on Visuospatial Attentional Reorienting in Non-Smoking Subjects. *Neuropsychopharmacology, 33,* 731-738.

Vossel, S., Thiel, C. M., & Fink, G. R. (2007b). Behavioral and Neural Effects of Nicotine on Visuospatial Attentional Reorienting in Non-Smoking Subjects. *Neuropsychopharmacology, 33,* 731-738.

Woolrich, M. W., Beckmann, C. F., Nichols, T. E., & Smith, S. M. (2009). Statistical Analysis of fMRI Data. In *fMRI Techniques and Protocols* (41 ed., pp. 179-236).

Yugar-Toledo, J.C., Ferreira-Melo, S.E., Sabha, M., Nogueira, E.A., Coelho, O.R., Consoline Colombo, F.M., Irigoyen, M.C., & Moreno Jr, H. (2005). Blood pressure circadian rhythm and endothelial function in heavy smokers: acute effects of transdermal nicotine. *Journal of Clinical Hypertension, 7*, 721-728.

FIGURE LEGENDS

Figure 1. Effects of nicotine on subjective experience of withdrawal. Mean scores (+ SEM) from the Modified Minnesota Withdrawal Symptom (MMWS) questionnaire administered immediately after scanning (N = 15, * P<0.05).

Figure 2. Effects of nicotine on behavioural measures of task performance. Top panel: Mean (+SEM) percentage of correctly identified targets. **Bottom panel:** Mean (+SEM) response time (in ms) to correctly identify targets. (N = 15, * P<0.05).

Figure 3. Brain regions of alpha-correlated activation and deactivation during RVIP performance. A. Orange/yellow depicts regions of alpha-correlated activation for the RVIP – CNTRL contrast. Blue depicts regions of alpha-correlated deactivation for the RVIP – CNTRL contrast. Group analyses were carried out using a mixed effects analysis with a corrected maximum height threshold of P<0.005. **B.** and **C.** Mean (+SEM) normalised % BOLD signal change for the contrast RVIP – CNTRL in each ROI at each visit (N=15). THAL = thalamus, dlPFC = dorsolateral prefrontal cortex, dACC = dorsal anterior cingulate cortex, PAR = parietal cortex, Angular gy = angular gyrus, PCC = posterior cingulate cortex, vmPFC = ventro-medial prefrontal cortex.

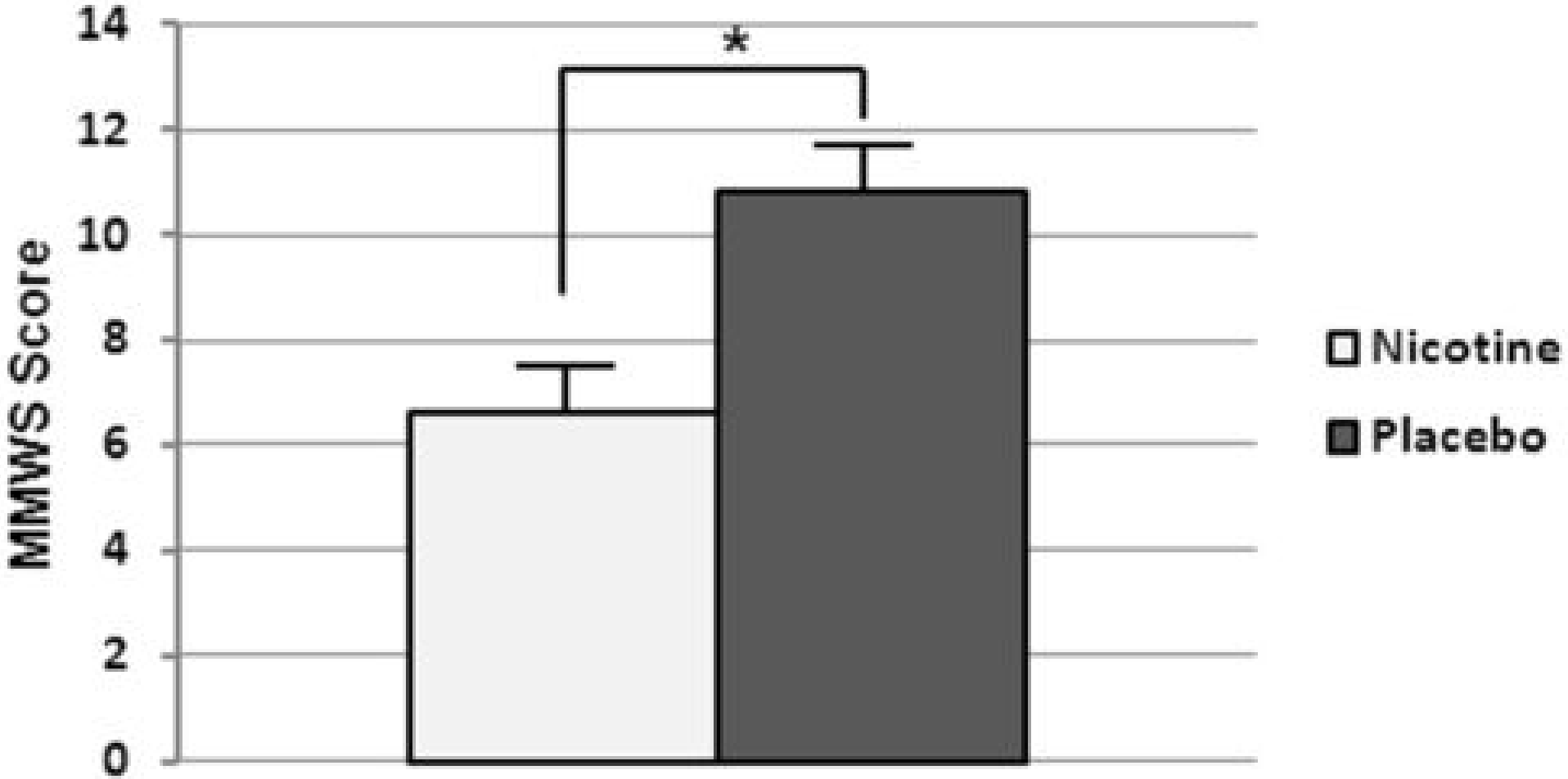
14
12
10
8
6
4
2
0
MMWS Score
*
Nicotine
Placebo

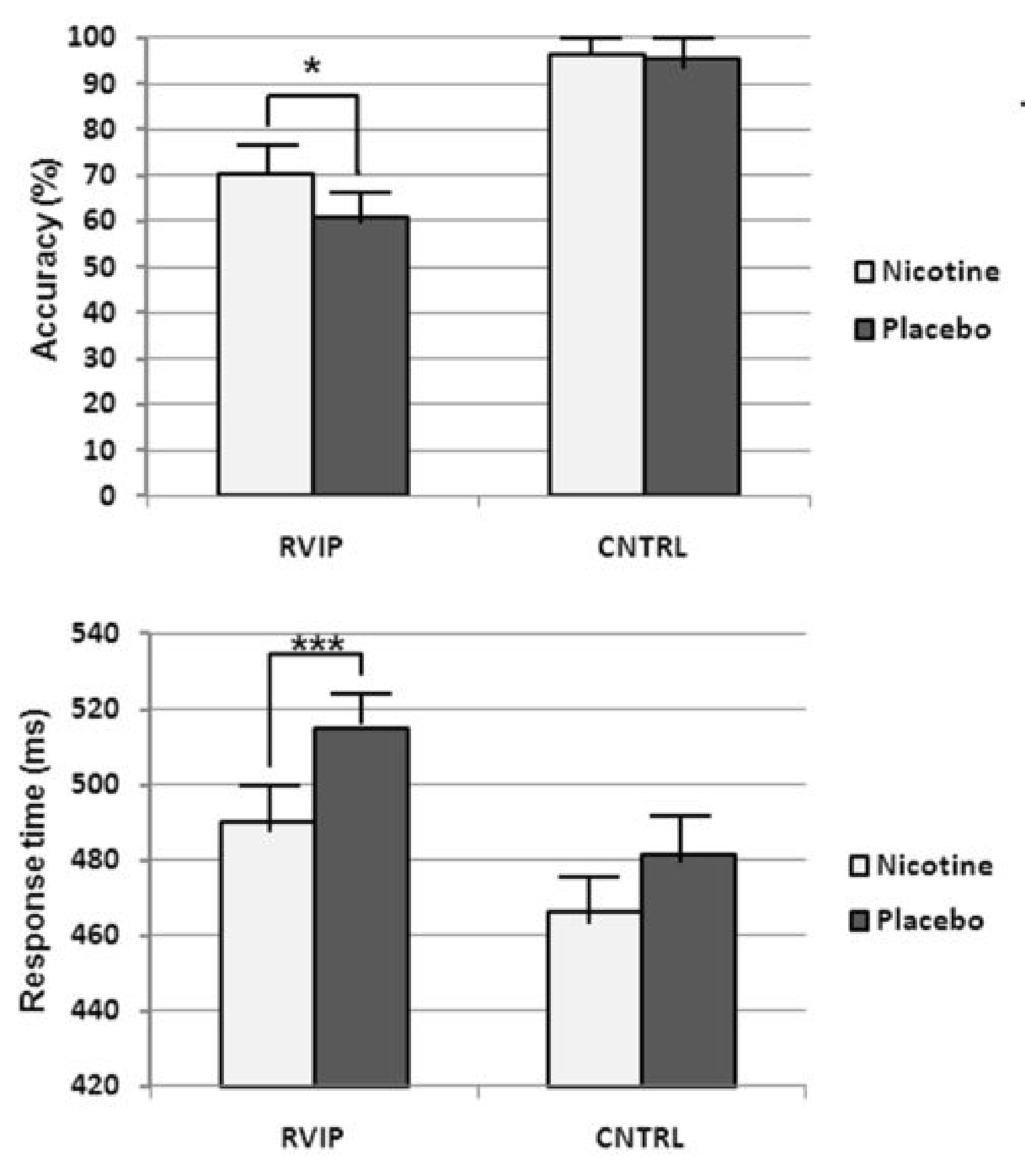
100
90
80
70
60
50
40
30
20
10
0
Accuracy (%)
*
RVIP
CNTRL
Nicotine
Placebo
540
520
500
480
460
440
420
Response time (ms)
***
RVIP
CNTRL
Nicotine
Placebo

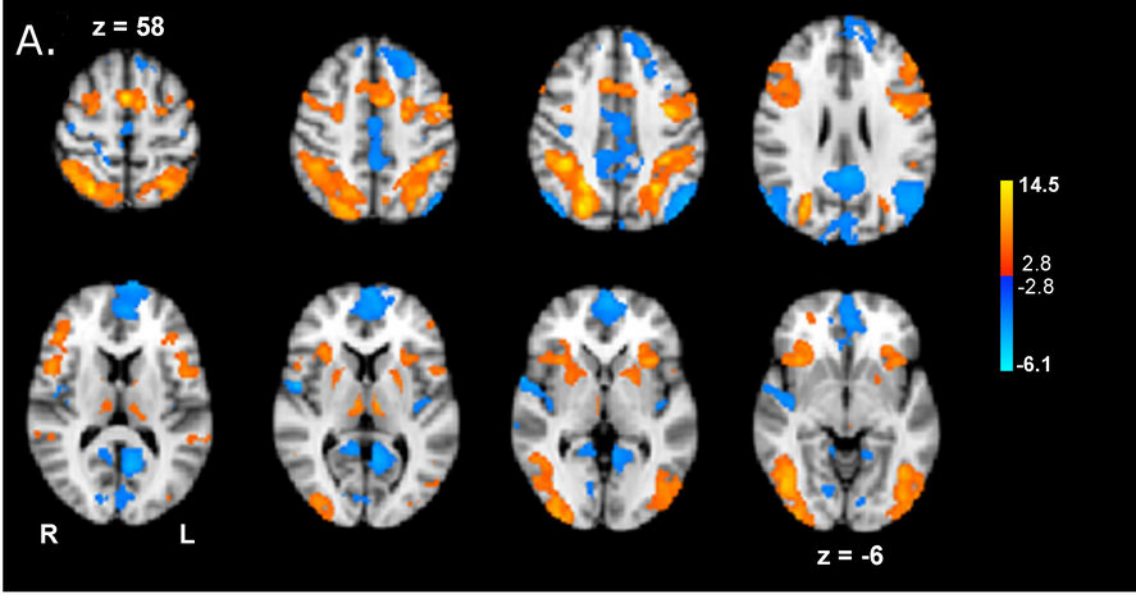
A.
z = 58
14.5
2.8
-2.8
-6.1
R
L
z = -6

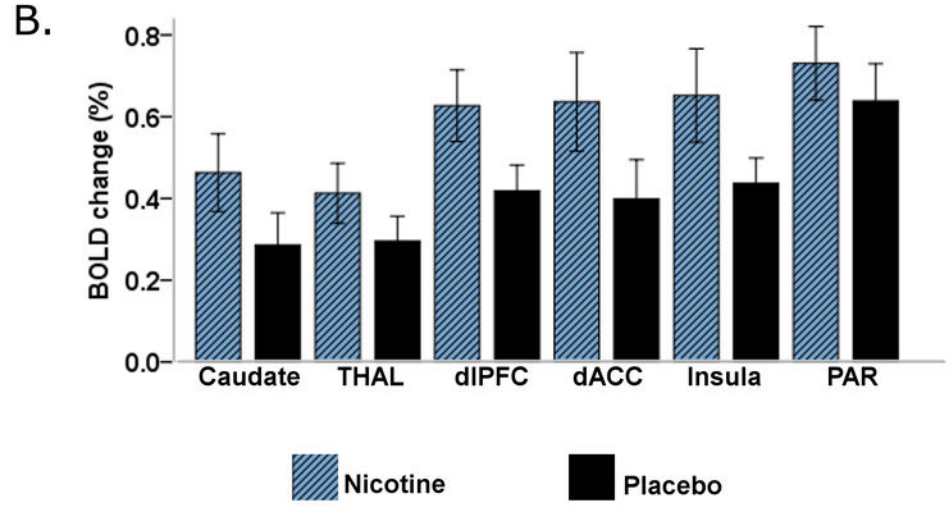
B.
BOLD change (%)
0.8
0.6
0.4
0.2
0.0
Caudate
THAL
dlPFC
dACC
Insula
PAR
Nicotine
Placebo

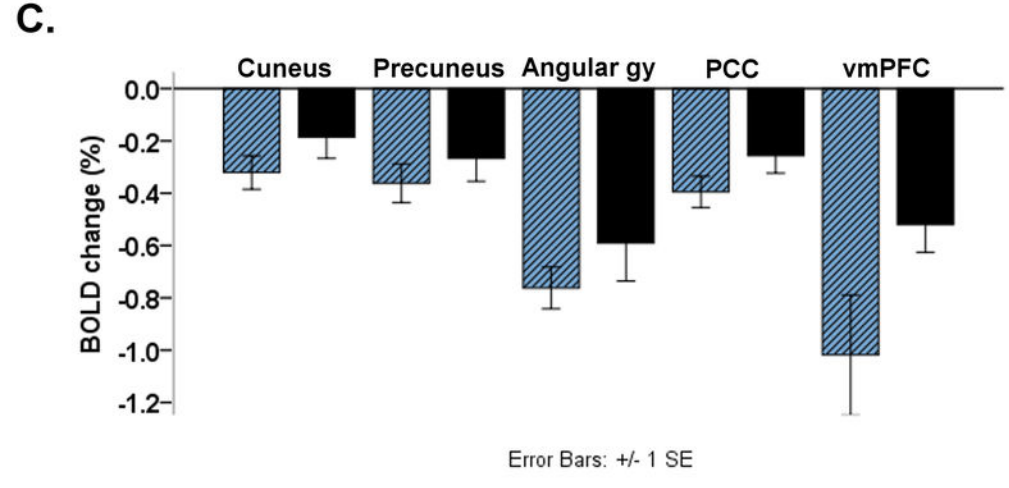
C.
Cuneus
Precuneus
Angular gy
PCC
vmPFC
BOLD change (%)
0.0
-0.2
-0.4
-0.6
-0.8
-1.0
-1.2
Error Bars: +/- 1 SE